Journal of Structural Geology 32 (2010) 1201–1211

Contents lists available at ScienceDirect

Journal of Structural Geology

journal homepage: www.elsevier.com/locate/jsg

Modeling fracture porosity evolution in dolostone

Julia F.W. Gale [a,*], Robert H. Lander [b], Robert M. Reed [a], Stephen E. Laubach [a]

[a] Bureau of Economic Geology, Jackson School of Geosciences, The University of Texas at Austin, University Station, Box X, Austin, TX 78713-8924, USA
[b] Geocosm LLC, 3311 San Mateo Drive, Austin, TX 78738, USA

ARTICLE INFO

Article history:
Received 27 February 2008
Received in revised form
16 October 2008
Accepted 9 April 2009
Available online 13 May 2009

Keywords:
Cement growth
Diagenesis
Dolomite
Opening-mode fracture

ABSTRACT

Opening-mode fractures in dolostones buried to depths of ~1–5 km contain synkinematic dolomite cement, the amount and internal structure of which has a systematic relationship to fracture size. Narrow fractures (<0.01 mm) typically seal completely with either massive cement or cement with a crack-seal texture that indicates multiple incremental openings. Wider fractures can preserve considerable effective porosity, but anomalously thick dolomite cement bridges are commonly present in fractures that are otherwise lined with a thin veneer of cement. Dolomite bridges resemble quartz bridges that are common in fractured sandstones.

We developed a geometric crystal growth model for synkinematic dolomite fracture fill in fractured dolostones, where periodic incremental fracture-opening events are introduced with concurrent cement growth. We assumed constant temperature and supersaturation with respect to dolomite. A key assumption in the model is that rapid dolomite accumulation within bridges is governed by high cement-growth rates on repeatedly broken grain surfaces during the process of crack seal. Slower cement-growth rates occur on euhedral crystals. This assumption is made on the basis of a comparison with quartz cement growth in fractured sandstones. Simulations with different fracture-opening rates mimic bridge and lining cement morphologies, including characteristic rhombic shapes of dolomite bridges.

1. Introduction

Opening-mode fractures have an important influence over fluid flow in many dolostones (e.g., Montañez, 1997; Antonellini and Mollema, 2000; Gale et al., 2004; Philip et al., 2005; Kosa and Hunt, 2006). The essential attribute for fluid flow is that fractures are open in the subsurface. Contrary to expectations of some fracture mechanical modeling, which predicts that subsurface loading conditions should close most large fractures (Zoback, 2007), core studies show that in dolostones, open fractures exist at depths up to 5 km (Gale et al., 2008) (Fig. 1). The stability and persistence of open fractures may reflect the stiffening effect of cements in host-rock pore space and isolated cement deposits within fractures (Laubach et al., 2004a). Here we investigate how such isolated cement deposits may form in dolostones.

Much published work on fractured carbonates has focused on conditions leading to fracturing and fracture reactivation, including the roles of effective stress, fluid pressure and confining pressures (e.g. Mollema and Antonellini, 1999; Hilgers et al., 2006). There has also been much work on carbonate mechanical stratigraphy (Corbett et al., 1987; Ferrill and Morris, 2008), and on the properties of carbonate fault rocks (Agosta et al., 2007). Core-based studies have highlighted the important role of cement in closing fractures and reducing dolostone fracture permeability (Gale et al., 2004), effects that have been quantified in elastic fracture mechanical and flow modeling of fracture patterns with cement modification (Philip et al., 2005; Olson et al., 2007).

Cementation in a fracture can be separated into synkinematic and postkinematic deposits, depending on whether the cement precipitated while fractures were opening or after the opening process had ceased (Laubach, 1988). The purpose of this paper is to provide insight into synkinematic cement deposition mechanisms in dolostone fractures through microstructural analysis and modeling. We use examples from the Lower Ordovician Knox Group in Mississippi, the Lower Ordovician Ellenburger Formation in West Texas, and the Pennsylvanian Canyon Group in New Mexico. Our geometric crystal growth model for synkinematic dolomite fracture fill in fractured dolostone is a modification of a model (*Prism2D*) that simulates quartz cementation in sandstones (Lander et al., 2008). The key process modeled is the differential cement-growth rate on euhedral versus broken nucleation surfaces, as repeated episodes of crystal breakage occur during

* Corresponding author. Tel.: +1 512 232 7957; fax: +1 512 471 0140.
E-mail address: julia.gale@beg.utexas.edu (J.F.W. Gale).

0191-8141/$ – see front matter © 2009 Elsevier Ltd. All rights reserved.
doi:10.1016/j.jsg.2009.04.018

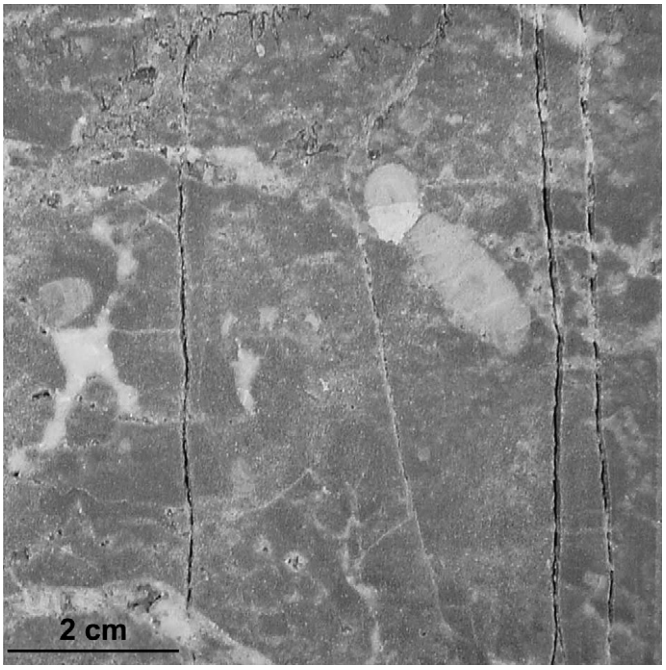

Fig. 1. Opening-mode fractures in Pennsylvanian dolostone core from 2370 m depth. Most fractures in this sample are partly open. Variability in the degree of openness is linked to total fracture width (kinematic aperture), with wider fractures being more open. Fracture porosity is partly occluded by dolomite cement bridges and linings.

incremental fracture opening (Lander et al., 2008). Growth rates on broken surfaces tend to be higher than predicted by the growth kinetics as noted in laboratory experiments with the analogue material alum (Nollet et al., 2006).

Following work in sandstones by Walderhaug (1994, 1996, 2000) and Lander and Walderhaug (1999), we infer that cement precipitation in dolostones, rather than material transport, governs dolomite accumulation rates. With this assumption, and the insight that cement accumulation rates differ on fractured and euhedral mineral surfaces (Lander et al., 2008), we predict cement deposit geometries that can be compared to natural examples.

2. Rates of fracture opening and cement precipitation

2.1. Rates of fracture opening

Sealing of opening-mode fractures during a phase of fracture growth can be thought of as a competition between the rates of fracture opening and synkinematic cement precipitation. As a result of this competition cements may fill the fracture completely, they may be present only as thin linings coating the fracture walls, or they may bridge across the fracture from one wall to the other. Cement bridges potentially contain much information on rates. In quartz systems, for example, fluid inclusion data from distinct crack-seal events in cement bridges provide information on the temperature during precipitation. As growth rate is dependent upon temperature, it is possible to calculate the growth rates on successive fracture surfaces. The growth rates, together with the kinematic aperture of each filled microfracture in the cement bridge, can then be used to calculate fracture-opening rates (Becker et al., 2008). Parris et al. (2003) used fluid inclusions from ankerite cements to constrain timing of fracturing events but did not investigate rates. The relative and absolute rates of fracturing and cement growth in the dolomite system remain poorly constrained or unknown. However, for bridges to form, the overall rate of fracture growth (in multiple opening increments) must be comparable to the rate of cement precipitation. We simulated several different relative opening-rate to cementation-rate ratios, to represent a range of situations, from those where cementation proceeds more quickly than fracture opening, to those where fracture opening is dominant.

Fractures accommodating opening displacement propagate along a plane of zero shear stress in isotropic rock, oriented perpendicular to the least compressive principal stress (Lawn and Wilshaw, 1975). This configuration makes fractures indicators of past stress orientations, but provides little information on the conditions that drive fracture growth. Fractures widen through some combination of diminished minimum stress and elevated pore fluid pressure. In our examples, synkinematic cement only spanned fractures in limited areas. Cement deposits must therefore be reacting to fracture opening rather than causing opening, for example by force of crystallization. Information on fracture rates would provide an essential constraint on conditions of fracture growth. Our model does not specify the loading conditions that drive fracture growth. Opening is represented as a uniform but incremental widening. We did not model the crack tip or reactivation in shear, which is a more complex situation, because comminution would need to be considered in addition to cement growth.

2.2. Precipitation rate laws

In an experimental study, Arvidson and Mackenzie (1999) determined that the precipitation rate of dolomite can be modeled with a rate law that is a function of saturation index,

$$r = k(\Omega - 1)^n \tag{1}$$

where r is the rate of precipitation per unit area, Ω is a unitless supersaturation term for ideal dolomite, and n is the order of the overall reaction. The rate term, k, takes an Arrhenius form:

$$k = A\, e^{(-Ea/RT)} \tag{2}$$

where A is a constant, Ea is the activation energy for dolomite precipitation, R is the real gas constant, and T is temperature.

Walderhaug (2000) recognized that temperature is the primary control for quartz precipitation; he used Eq. (2) to model quartz cementation and porosity loss in sandstones. Lander et al. (2008) noted that the supersaturation term is implicit in A because the fluid in sandstone reservoirs is at or above saturation with respect to quartz. We follow a similar line of argument for dolomite. We model the precipitation of dolomite in a fractured dolostone from a fluid supersaturated with respect to dolomite. Although stylolites are present in some samples (e.g. Fig. 1), we found no evidence of dissolution of fracture-filling cements in our examples. We therefore contend that confining our modeling to precipitation is geologically reasonable for some cases.

Although it would be desirable to model actual precipitation rates in the dolomite system using the above equations, a key piece of information is missing. We do not know the relative precipitation rates on broken versus euhedral surfaces. We assumed a strong rate differential, as is the case for quartz (Lander et al., 2008).

3. Mechanisms of fracture sealing – previous work

3.1. Synkinematic cement

Crystal growth in syntectonic crack-seal veins was described by Hilgers and Urai (2002a), and simulated numerically on the basis of a kinematic model (Bons, 2001; Hilgers et al., 2001). The aim of these simulations was to investigate processes in completely sealed

veins, where repeated breakage occurs along the length of the vein. The aforementioned authors were particularly interested in mechanisms controlling the development of fibrous morphology and, consequently, in how fibres might follow a fracture-opening trajectory. Hilgers et al. (2001) listed several controlling factors including fracture-opening velocity, grain size, wall roughness, growth anisotropy and crystal growth velocity. They found that "grain boundaries track the opening trajectory if the wall roughness is high, opening increments are small and crystals touch the wall before the next crack increment starts". However, their simulations did not attempt to replicate variation of fracture porosity with fracture size, or with respect to mineral bridges. Brantley et al. (1990) found experimentally that small fractures tend to seal more rapidly than large ones and concluded that this is because narrow-aperture fractures have a large surface area relative to their volume. While this conclusion is generally true, it does not explain the development of mineral bridges.

3.2. Postkinematic cement

Porosity-reducing cements in large opening-mode fractures are commonly postkinematic (Gale et al., 2004). The distribution of postkinematic cements is generally heterogeneous, which might reflect variations in flow pathways and compositions of late fluids (Laubach, 2003). Mechanisms controlling postkinematic cement growth of dolomite are probably different from those that control synkinematic cement growth. This difference arises because fresh surfaces are no longer being generated by fracturing. Experimental and numerical modeling investigation of syntaxial vein growth by Hilgers et al. (2001), Noh and Lake (2002), Hilgers and Urai (2002b) and Nollet et al. (2005, 2006) may replicate aspects of post-kinematic growth. These studies emphasized the importance of advective or diffusive transport, degree of supersaturation, and crystal growth competition. The growth rate of crystals is influenced by depletion of solute along the fracture length, and growth competition is controlled by crystallographic orientation, crystal size, and crystal location.

3.3. Fracture population size statistics, cement and porosity

In rocks with power-law fracture size-distributions (Marrett et al., 1999), narrow fractures are relatively numerous and can accommodate significant amounts of strain (up to 5% in Cretaceous Cupido Formation dolostones in NE Mexico, J. Gale, unpublished data; Gomez and Laubach, 2006). Because sealing is size-dependent, the size distribution of the population and the break-over size (termed *emergent threshold* by Laubach (2003)) from sealed to open fractures governs overall fracture porosity. Break-over aperture sizes of less than 0.1 mm have been observed in fractured dolostones, meaning that appreciable porosity can be preserved in submillimeter fractures (Fig. 1) (Gale et al., 2004; Gale and Gomez, 2007). At this aperture size, however, cement linings and bridges are likely to limit within-fracture pore connectivity. At larger aperture sizes, linings are thinner than the open part of the fracture, and pores are more likely to be connected because there are fewer bridges. The interaction of mechanical and chemical (diagenetic) processes thus exerts a first-order control over the distribution of open fractures (Olson et al., 2007).

4. Geological setting

We examined fractures in dolostones from three different groups. In the Permian Basin of West Texas the Lower Ordovician Ellenburger Group comprises shallow-water dolostones and limestones. They are commonly brecciated by palaeokarst-related processes, but we studied late opening-mode fractures that post date the brecciation (Gale and Gomez, 2007). Ordovician Knox Group dolostones in Maben Field, Mississippi, comprise two depositional facies: a tidal-flat facies and a shallow, subtidal, carbonate platform. These form a series of stacked, fifth-order, high-frequency, upward-shoaling cycles. Natural open fractures, trending predominately N–S, may be associated with the Pennsylvanian age Ouachita thrust front, which ramps upward and over underlying horst and graben features of Paleozoic carbonates (Gale et al., 2008). Pennsylvanian Canyon Group dolostones, consisting of phylloid algal mounds and associated grainstones and

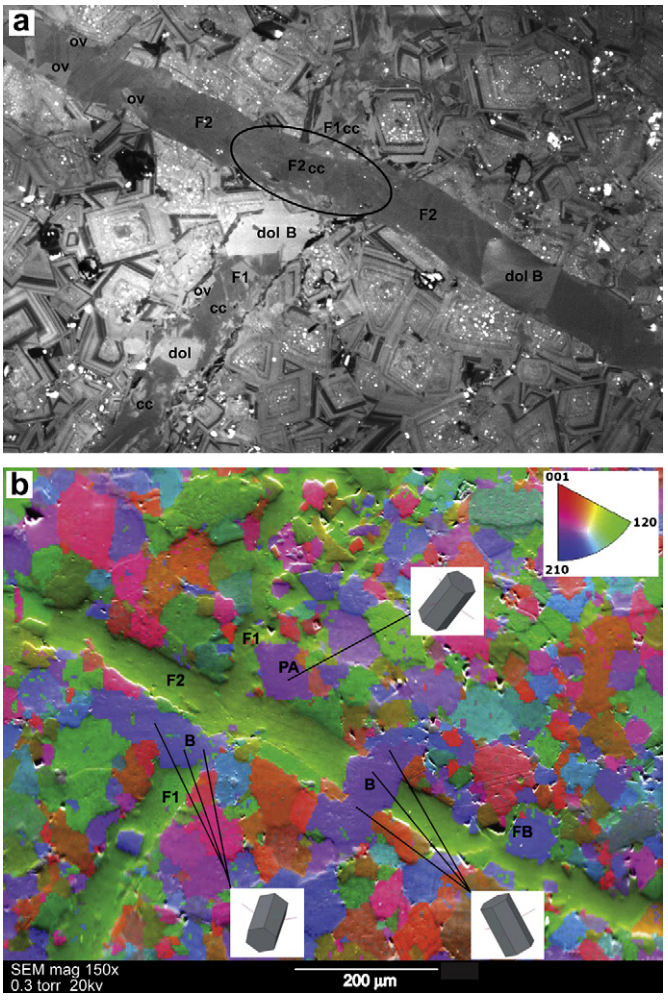

Fig. 2. Ordovician Knox Group dolostone from a depth of approximately 4444 m (14,580 ft) contains two sets of cross-cutting fractures, F1 and F2. (a) SEM-CL image showing dolomite (dol) is the first cement in each fracture set, forming overgrowths (ov) and bridges (B). Calcite (cc) is the second cement. The F2 fracture cross cuts the F1 fracture (ellipse). Both fractures are calcite filled at the cross-cutting location, but the two calcite cements have different CL signatures, F2 calcite being darker in the image (lower luminescence). (b) EBSD map of crystallographic orientation superimposed over an orientation contrast image, with spot analyses shown as crystal orientation diagrams. Noise reduction was used on the map. There are examples of bridges (B), where the sealing cement has templated onto a broken wall rock dolomite crystal and has the same crystallographic orientation. There are also examples of failed bridges (FB) where cement accumulation eventually did not keep up with fracture opening and locations where orientation of the host grain was favorable for a bridge to form, but where the fracture apparently propagated around the dolomite crystal (PA) instead of breaking through it. The calcite in both fractures (green) shares a common orientation. Inset shows inverse pole figure color key for calcite, which functions for both calcite postkinematic cement and dolomite. The inverse pole figure is relative to the z-axis of the image (out of plane).

packstones, form reservoirs in the northwestern part of the Permian Basin in New Mexico (Dutton et al., 2005). Open fractures are common in these rocks (Fig. 1) but the regional cementation history is complex. In some locations late anhydrite forms post-kinematic cement (J. Gale, unpublished data). Here we focus on dolomite cements only.

5. Microstructure observation

A combination of scanning-electron-microscope-based cathodoluminescence (SEM-CL), using a UV-blue filter to eliminate persistent luminescence streaking from carbonate minerals (Reed and Milliken, 2003), and secondary electron imagery (SEI) allowed us to examine cement microstructures and relict porosity. We used electron backscatter diffraction (EBSD) to measure crystallographic orientation of grains in fracture walls and cement crystals. An initial subset of imagery was used to guide model design and for comparison with model results; a second subset of imagery that became available after the modeling had been finished was used for comparison with model results.

A core sample of Knox dolostone from a depth of approximately 4439 m, revealed two approximately orthogonal opening-mode fracture sets with clear cross-cutting relationships (Fig. 2a). These were described in detail by Gale et al. (2004). In summary, the earlier fracture set (F1) is partly occluded by dolomite, which grew first, forms linings and bridges, and contains crack-seal texture. Later calcite occludes remaining pores in some fractures, whereas others retain some fracture porosity. Dolomite was also the first cement to precipitate in the later fracture set (F2), and was followed by a second, later calcite. Dolomite is consistently the first-formed cement in fractures in this and other samples, indicating that rock composition strongly influences initial cement composition: in dolostones the first-formed cement is typically dolomite, in sandstones it is quartz, while in limestones it is calcite. An EBSD map of this sample, recovered from a depth of about 4444 m, demonstrates that grains in fracture walls and adjacent cement crystals in the fractures have a common crystallographic orientation (Fig. 2b). As with quartz, nucleation of dolomite is greatly assisted by the presence of a dolomite substrate on which to grow.

Dolomite bridge structures in dolostones resemble quartz bridges found in sandstones (Laubach et al., 2004b, 2006). In both cases the mineral bridge consists of a continuous pillar of cement extending from one wall of the fracture to the other (Figs. 1–3). Adjacent to many bridges, fracture walls are coated by a veneer of small euhedral crystals, leaving the fracture largely open. The bridge may be composed of a single crystal (Figs. 2 and 3), or multiple crystals (Fig. 4). In dolostone, dolomite bridges tend to be rhomb shaped, whereas quartz bridges tend to be straight sided (Gale et al., 2004). Quartz bridges in sandstone typically contain many small sealed fractures, indicating that the bridge has formed through a crack-seal process (Laubach et al., 2004b, 2006). Dolomite bridges fall into three groups: (i) those with crack-seal texture across the whole bridge (Fig. 4a), (ii) those in which crack-seal texture has been overgrown by dolomite showing no further fracturing (Fig. 4b), and (iii) those with no apparent crack seal (Fig. 4c). Fractures completely sealed by dolomite may show crack-seal texture or may be sealed after a single opening event (Fig. 5a). The tips of large open fractures commonly taper and become sealed; they may show complex linking and branching where they grow together (Fig. 5b).

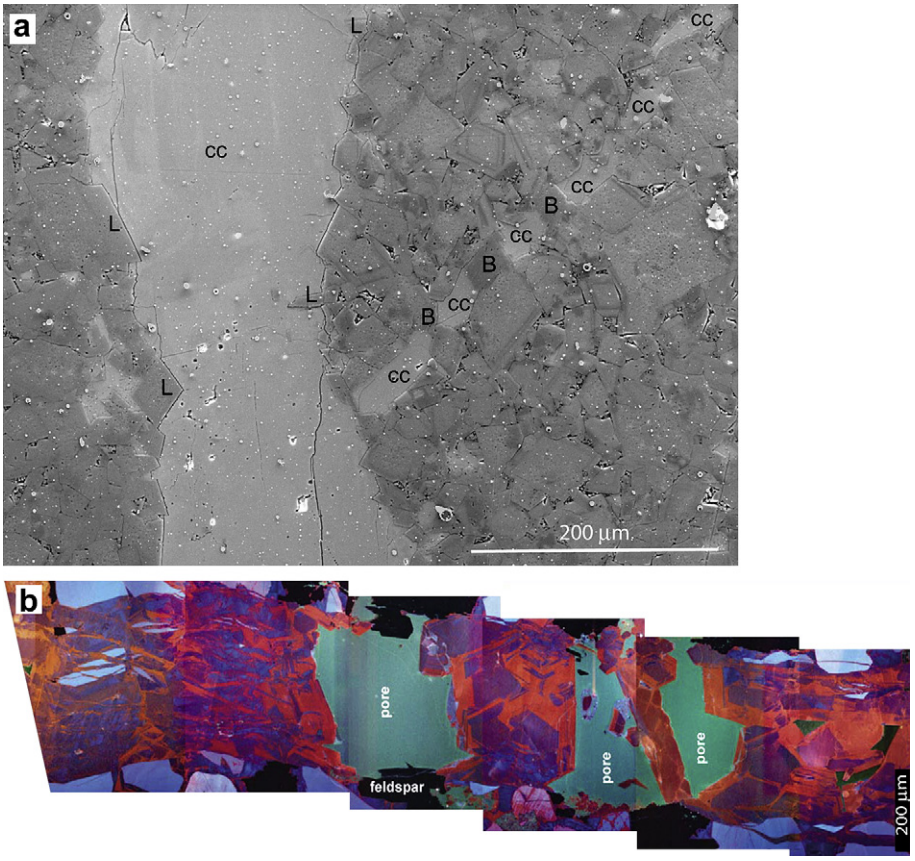

Fig. 3. (a) Superimposed SEM-CL and SEI images of fractured dolostone from Knox core from 4413 m showing calcite-filled fractures (pale grey, cc), dolomite bridges (B), and linings (dark grey, L) (b) SEM-CL image of quartz bridges in sandstone (from Laubach et al., 2004b, their Fig. 8).

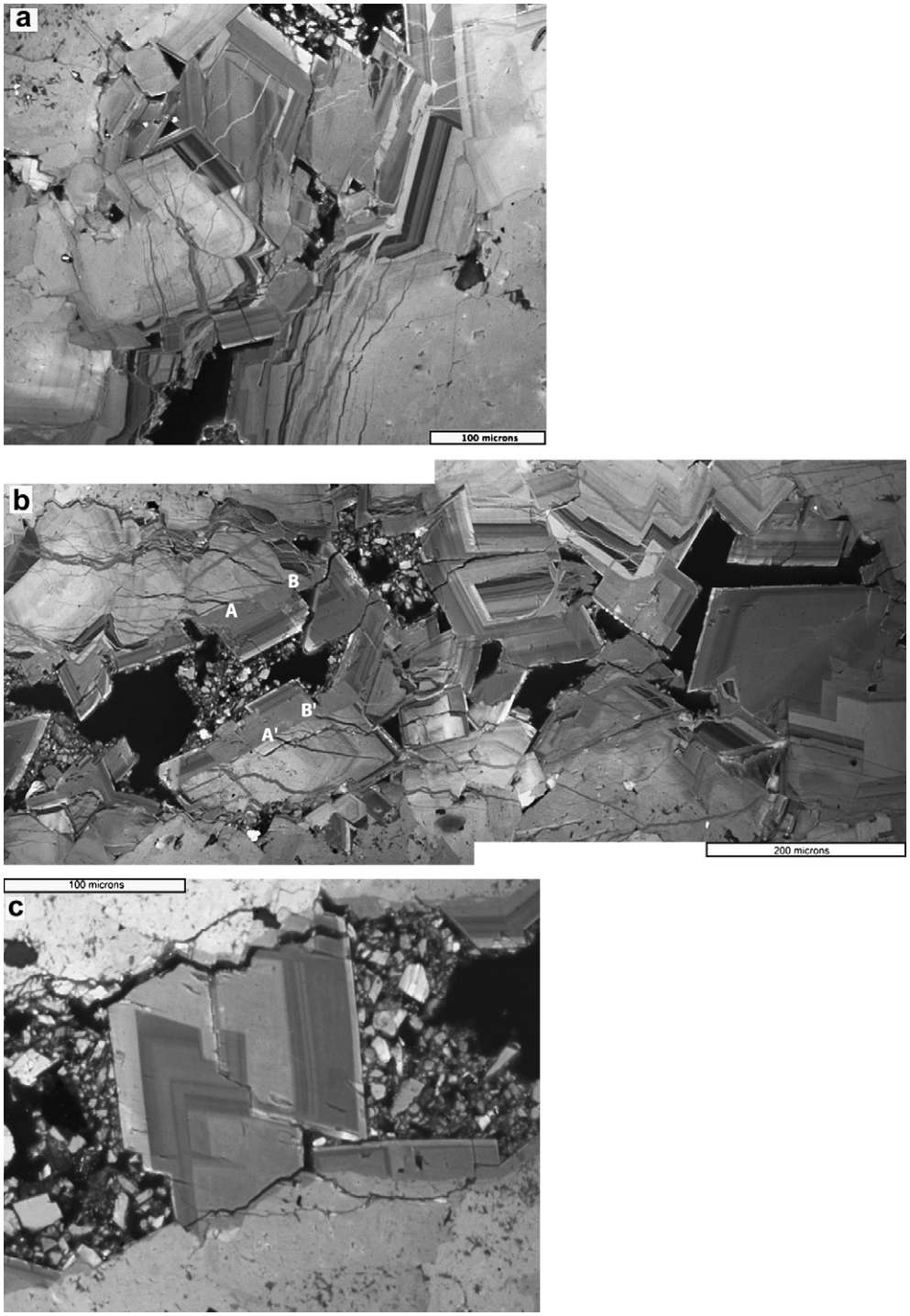

Fig. 4. SEM-CL images of microstructure in dolomite bridges. (a) Bridge with crack-seal texture developed across the whole bridge. The resulting bridge is composed of multiple crystals. (b) Failed bridge with early phase of crack-seal growth, followed by fracture opening and subsequent postkinematic cementation. Points A and B were joined to A′ and B′, respectively, during a time when this part of the fracture was bridged. (c) Bridge with no crack-seal structure. Growth zoning is uninterrupted and reflects continuous, probably postkinematic, growth.

6. Fracture sealing model

6.1. *Explanation of the* Prism2D *model*

The *Prism2D* model uses a continuous value cellular automata approach for simulating crystal growth geometries (Lander et al., 2008). Cells in a two dimensional orthogonal grid may be partly or completely filled by cement solids. Each cement cell has a specified crystal orientation and experiences growth rates that depend upon the available porosity, the spatial and crystallographic orientations of cements in neighboring cells (if any), and external controls such as temperature and degree of supersaturation. Experimental growth rates for different crystal surface types are used to constrain relative modeled growth rates. The most important effect is that growth on broken surfaces is 20 times faster than growth on euhedral faces.

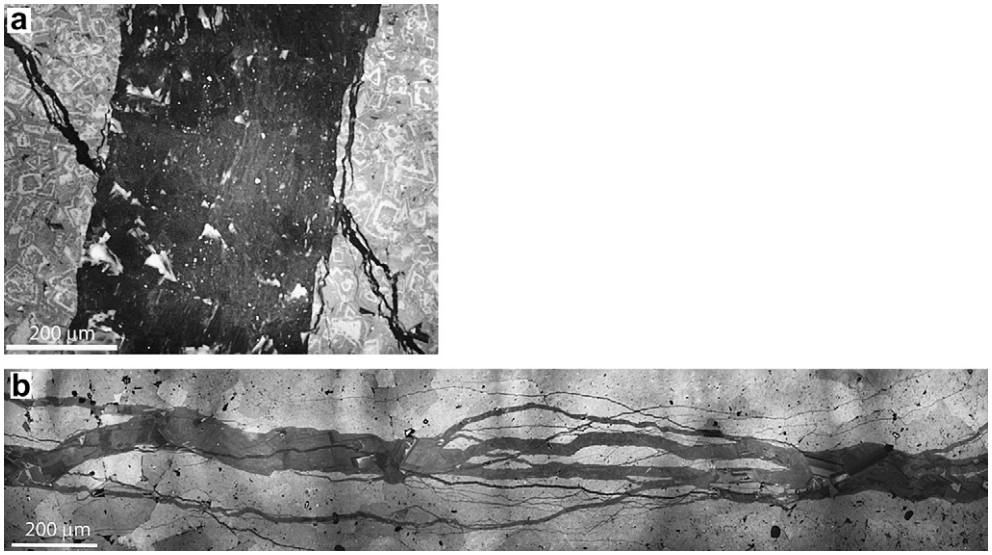

Fig. 5. Narrow fractures completely sealed by dolomite cement. (a) Sealed fracture with crack-seal texture showing slivers of wall rock entrained in fracture cement. (b) Multiple sealed branches at junction of two fracture tips.

6.2. Dolostone modeling

The first step was to make a model dolostone into which we could introduce opening-mode fractures. We made a framework of dolomite rhombs using SEM-CL and SEI images of a Knox Group dolostone (Fig. 6a, b). We then filled model template pore spaces with simulated dolomite cement, growing in crystallographic continuity with host grains, using the *Prism2D* forward cement-growth function. Small pores remain after this step (Fig. 6b). Modeled grain boundaries after this step resemble those in the natural example, in which original rhombs and later cements are hard to distinguish (Fig. 6c). The template (Fig. 6d) serves as a nucleation substrate for cement growth within a modeled fracture.

Different colors in the template signify different dolomite crystals in the host rock. Orientations of the long diagonal of crystal rhombs are described by an azimuth (orientation within the plane being simulated) and a bearing (angle with respect to the modeled plane). Azimuth orientations are restricted to N–S, E–W, NW–SE, and NE–SW directions, but the bearing may be set to any arbitrary angle. We conditioned cement growth to be in crystallographic continuity with crystals in fracture walls, in accordance with our EBSD observations (Fig. 2b). To represent this process in the model, the fracture cement was given the same color as the host grain.

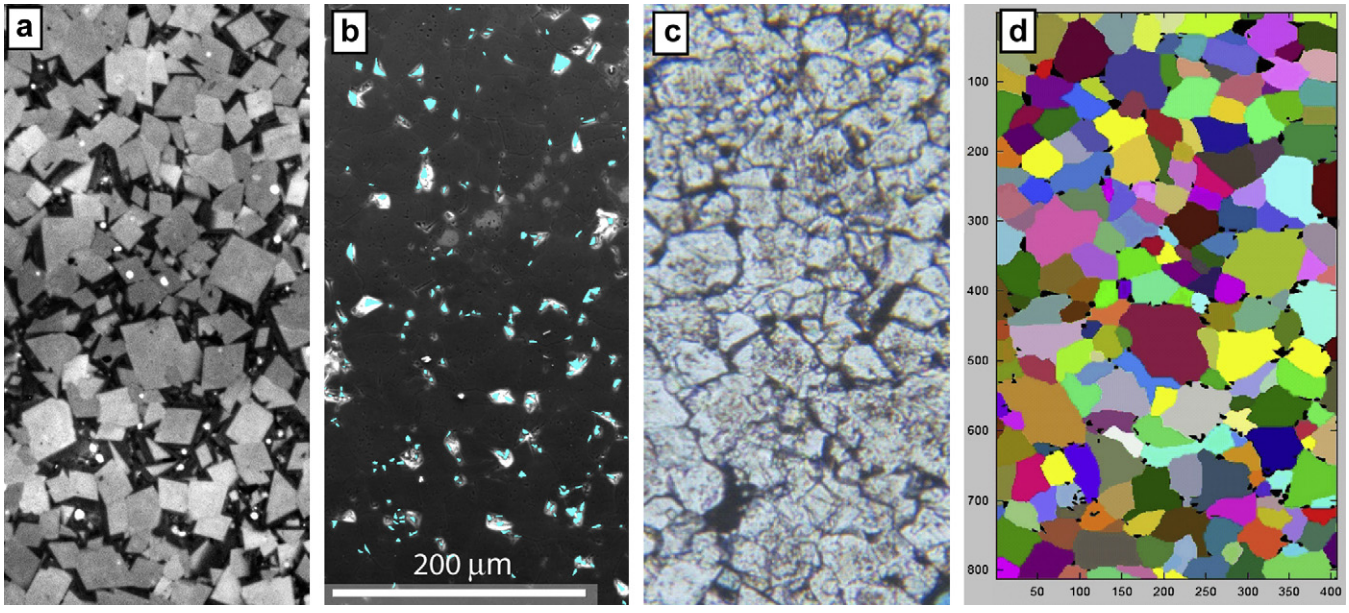

Fig. 6. Construction of model template. (a) SEM-CL image, (b) SE image where cyan highlighting indicates porosity, (c) plane light image of Knox dolomite sample, and (d) model template where the colors represent individual crystal domains and black shows porosity. The scale bar applies to all figure parts.

To simulate development of an opening-mode fracture in a model run, we extended the template laterally in constant size increments by inserting open columns in a contiguous vertical zone (Fig. 7). The location of the first fracture increment is set arbitrarily (in this case at column 150 of the template shown in Fig. 6d), and subsequent fracture locations are inserted at random in a zone that extends 10 columns on either side of the fracture boundaries. Only cement that is continuous across a fracture can break during an opening increment. We adjusted the frequency of insertion of the opening increments (microfractures) to simulate different rates of fracture opening. When a microfracture is introduced at a given model time-step, dolomite cement is allowed to grow into the fracture pore space during that time-step and from that point forward. We assume a constant temperature and supersaturation with respect to dolomite for all runs.

By analogy with quartz (Lander et al., 2008) we assume that the growth rate on broken surfaces is 20 times faster than the growth rate on euhedral surfaces. Sensitivity tests suggest that the absolute value of the growth-rate enhancement is not as important as its presence (Lander et al., 2008). Although there is some textural indication of small growth-rate differences on different dolomite crystal faces, these differences are probably small (Nordeng and Sibley, 1996; Rolf Arvidson, pers. comm., 2007). Indeed dolomite crystals are typically equant and our SEM-CL imagery did not reveal evidence of significant face-related growth anisotropy. We decided this effect is unlikely to have first-order control over cementation patterns, and for simplicity in the model we assumed equal growth rates on all crystal faces. This contrasts with quartz, where growth is significantly more rapid parallel to the c-axis (Lander et al., 2008, and references therein). Orientation of host-rock dolomite crystals is important, however, because it controls whether the fracture will break at an oblique or a more nearly parallel orientation with respect to euhedral faces. This breakage angle governs the amount of freshly broken surface that each fracture increment will produce.

Model runs were completed with different fracture-opening rates (Fig. 7). Each model run has 400 steps in total (a step represents the growth required to fill one model cell completely after nucleation on a broken surface). Fractures are allowed to grow during model steps 1–300. Different fracture-opening rates were modeled by allowing fractures to grow by increments of one in ten steps (slow growth rate; Fig. 7a, b), one in four steps (moderate growth rate; Fig. 7d, e), every other step (fast growth rate; Fig. 7h, i), and every step (very fast growth rate; Fig. 7k, l). Cementation proceeded at every step in all models. Relative cement-growth rates are represented in model results with red for fast growth on broken surfaces, and green for slow growth on euhedral surfaces (second column in Fig. 7). Our model also allows postkinematic dolomite to accumulate after the fracture ceases to open, during steps 300–400, but does not account for heterogeneous deposits of postkinematic calcite and other phases.

7. Comparison of model results with microstructure observations

Relative rates of cement growth and fracture opening govern the transition from sealed (Fig. 7a–c) to open fractures (Fig. 7d–m), and determine whether fractures above the break-over size are bridged (Fig. 7d–j) or merely lined by a thin veneer of euhedral crystals (Fig. 7k–m). If fracture opening is interrupted after only a few small increments, postkinematic dolomite will seal the small aperture fractures, showing that fracture size also governs fracture porosity preservation. This result is consistent with our observation of numerous, completely dolomite-sealed microfractures in our examples.

7.1. Slow opening-rate model

In this model scenario, the fracture-opening rate is slower than the slowest dolomite cement-growth rate. Each fracture-opening event is consequently small enough to be sealed before the next fracture event. The result is a completely sealed fracture with cement that is in crystallographic continuity with the wall rock (Fig. 7a). In cases where final fracture width is of the order of the grain size of the host rock, such fractures may be difficult to detect without the use of SEM-CL, as illustrated by model results in Fig. 7a. The modeled fracture typically has zones of fast (red) and slow (green) growth, reflecting whether the fracture trace is at a high angle or more nearly parallel to the orientations of euhedral crystal faces, respectively (Fig. 7b). Natural examples of fractures completely sealed by dolomite are common (Fig. 7c).

7.2. Moderate opening-rate model

Fracture-opening rate in this simulation is faster than cement growth on euhedral surfaces but slower than growth on fractured surfaces. Dolomite crystals with euhedral growth faces at an oblique angle to the fracture trace thus experience fast growth when they are fractured. This growth is sufficiently fast for these crystals to grow across the microfracture between fracturing events. The geometry perpetuates itself as new fracture events break the bridged crystal, creating more fast-growing, broken surfaces. By contrast, crystals with euhedral faces subparallel to the fracture trace become euhedral very quickly after fracturing and grow into the fracture at rates that are too slow to seal the fracture. Consequently, these crystals are not broken by subsequent fracturing events. With progressive fracturing, crystals having oblique face geometries make up an increasing proportion of the fracture fill because of their faster net growth rates. This simulation produces dolomite bridges and elongate, straight-sided pores with narrow dolomite linings (Fig. 7d, e). In the natural fracture example, similarly shaped pores occur where rhomb faces are subparallel to fracture walls (Fig. 7f, g).

7.3. Fast opening-rate model

As with the previous model scenario, the fracture-opening rate is faster than cement growth on euhedral surfaces and slower than growth on broken surfaces. The faster fracture-opening rate, however, means that fewer crystals are oriented favorably to grow across the fracture between fracture events. These few crystals are more likely to develop a euhedral growth form because of limited growth competition among bridging crystals. Large rhomb-shaped dolomite bridges are thus more prevalent in this simulation (Fig. 7h, i) than in the slower bridging model (Fig. 7d, e). Fracture pores also tend to become less slot-like owing to the larger kinematic aperture of the fracture itself (Fig. 7h, i). Rhomb-shaped bridges are present in natural fractures (Figs. 4 and 7j) and may result from continued crack seal (this simulation and natural example in Fig. 4a) or initial crack seal followed by postkinematic growth (Figs. 4b and 7j). The models predict that fracture-normal panels of competing crystals will make up some larger rhomb-shaped bridges.

7.4. Very fast opening-rate model

In this simulation, rate of fracture opening outstrips even the fastest rate of crystal growth so that no crystal can bridge the fracture between fracturing events (Fig. 7k). If bridges do not form initially, then no new fracture surfaces are created during the next fracture increment, and, consequently, growth slows owing to the

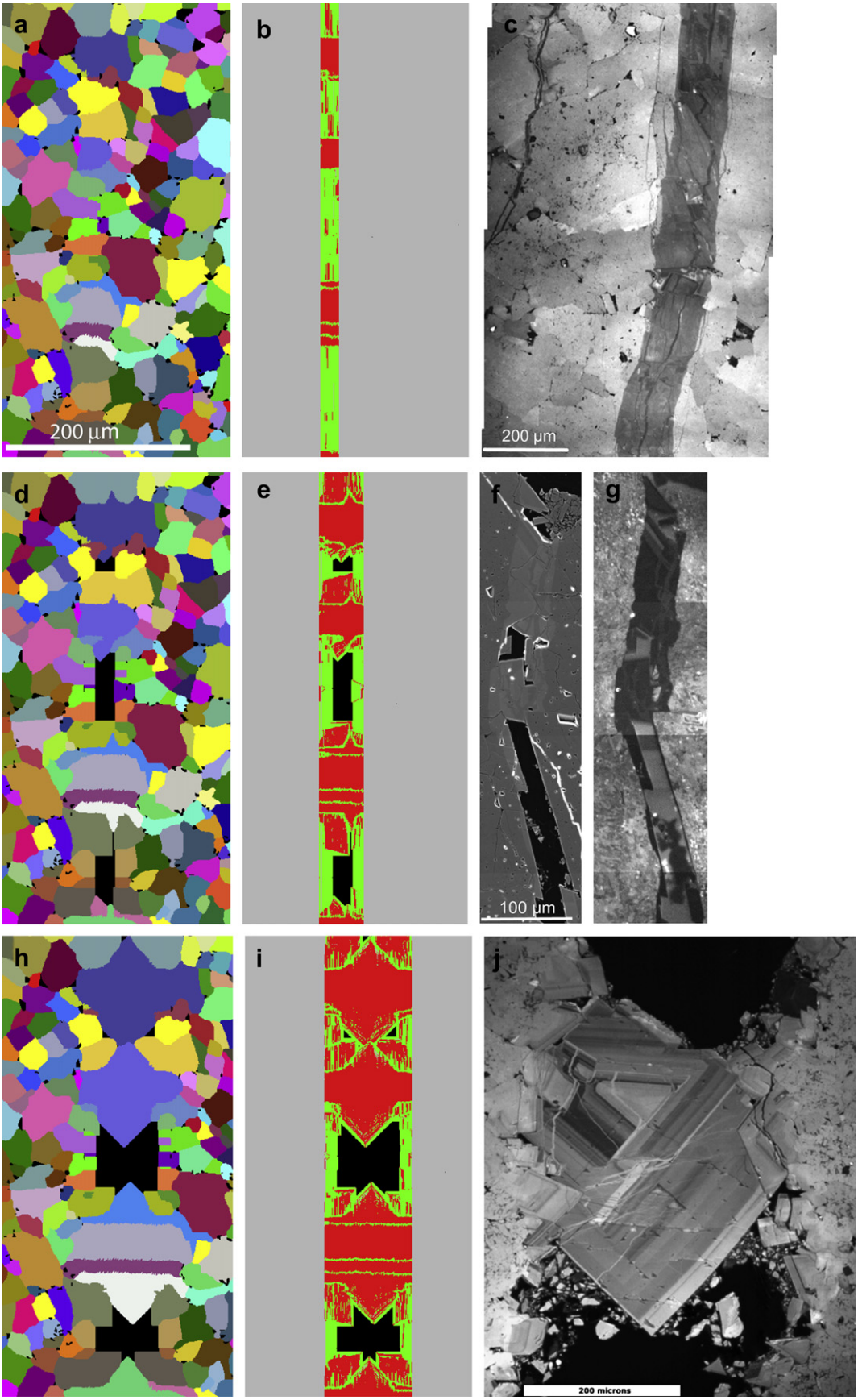
a
200 μm
b
c
200 μm
d
e
f
100 μm
g
h
i
j
200 microns

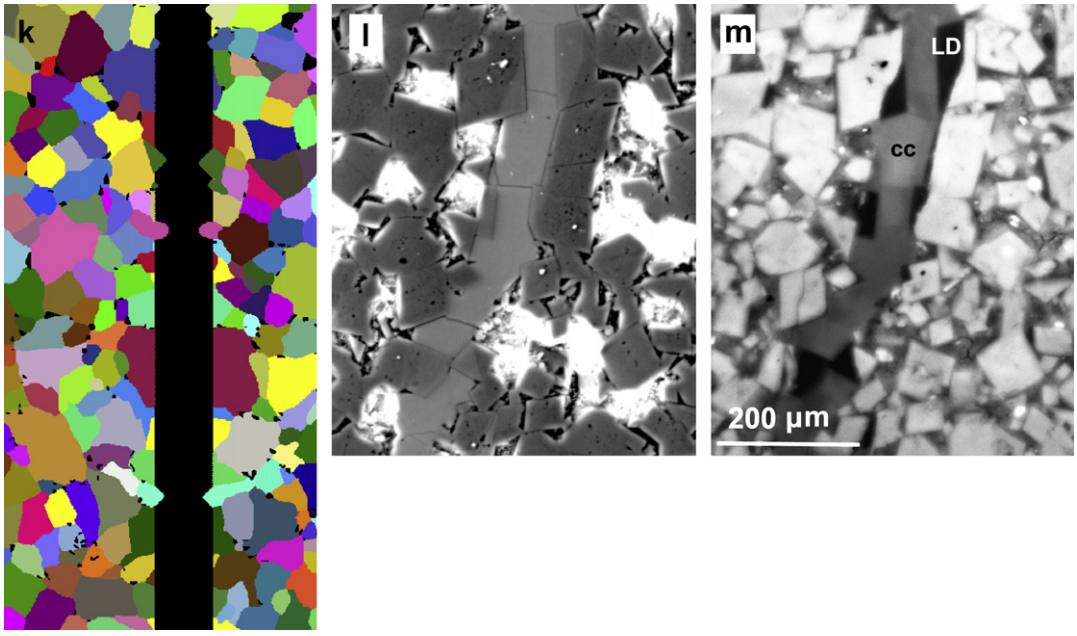

Fig. 7. (*continued*).

lack of broken surfaces. Even crystals that are fractured oblique to rhomb faces, on which growth is relatively fast, fail to grow across the break and quickly become euhedral (Fig. 4k–m). An additional ramification for this model scenario is that it results in reduced absolute cement volume within the fracture as compared with the two bridge scenarios, despite having a larger open volume for potential cement growth. Natural examples of fractures having a veneer of faceted dolomite are common in core, suggesting that fracture-opening rates commonly outstrip dolomite accumulation rates.

7.5. Multiple sealing styles in a single sample

In the Pennsylvanian dolostone core sample in Fig. 1, many of the sealing styles described earlier are present within a single thin section, reflecting a population of different fracture sizes (Fig. 8). Where fracture-opening rate was slow enough to allow complete sealing of the fracture after each fracturing event, the end result is a completely sealed fracture. Narrow tips of otherwise wider fractures show complete sealing, which we interpret as a result of slower opening rates at fracture tips. Where the fracture-opening rate was faster, some dolomite cement was able to bridge the fracture aperture. In simulations discussed earlier, although there are no initial differential rates among euhedral faces, bridges form because rhomb faces that are parallel to crystal walls become euhedral more quickly than those at an angle to the walls. Failed bridges occur where fracture events delineated by crack seal maintained a fast cementation rate initially but were subsequently unable to prevent the crystal from becoming euhedral (Fig. 4b). These crystals commonly have rhomb faces that are subparallel to fracture walls. Complex growth textures can arise as a result of competing growth on adjacent crystals and difference in growth rate on euhedral versus anhedral surfaces. Differences in growth rate may give rise to different CL signatures as CL-quenching or CL-enhancing ions become more or less incorporated into the crystal structure.

8. Discussion

Our results for cement distribution and morphology in fractures differ markedly from results obtained by Hilgers et al. (2001), Noh and Lake (2002), Hilgers and Urai (2002b) and Nollet et al. (2005, 2006) because of several factors. The most important factor is that we incorporated differential cement precipitation rates on broken versus euhedral surfaces. Second, we treated precipitation, rather than material transport, as the rate-limiting step. Third, we modeled fractures as evolving in multiple opening increments with continuous cementation, rather than as a single open fracture passively sealing after it has ceased opening. Results also differ from previous modeling of crack-seal in completely sealed veins (Hilgers and Urai, 2002a; Bons, 2001; Hilgers et al., 2001) because there is no fracture porosity in those systems. We therefore see this contribution as being complementary to previous work on fracture sealing. Recognition of the controlling processes in different situations is fundamental to being able to explain and predict the morphology of, and extent of fracture filling by, synkinematic cements.

The relationships between fracture-opening rate, cementation rate, and porosity preservation have implications not only for hydrocarbon reservoir permeability, but also for understanding the development of fracture systems in general. If dolomite accumulation rates on fractured and euhedral surfaces could be obtained,

Fig. 7. Model appearance after simulation showing crystal domain geometries (column 1) and cement-growth rates (column 2) together with corresponding natural examples of cement microstructure (columns 3 and 4) for four different fracture-opening rate simulations. (a–c) Slow opening-rate simulation resulting in completely sealed fractures. The scale bar in (a) applies to all models. (d–g) Moderate opening-rate simulation resulting in bridge structures where growth is fast and slot-shaped pores associated with maintained fast cement-growth rate. (h–j) Fast opening-rate simulation resulting in rhomb-shaped bridges. (k) Very fast opening-rate simulation where cement growth was too slow to keep up with opening rates and no crystals bridged across. (l) SEI and (m) SEM-CL of Ellenburger dolostone sample showing that dolomite sealing of fracture was incomplete. Low-luminescent dolomite (LD) overgrowths vary in thickness according to crystal orientation. They contain slightly more iron and less magnesium than the other dolomite (Gale and Gomez, 2007). Fracture is sealed by postkinematic calcite (cc).

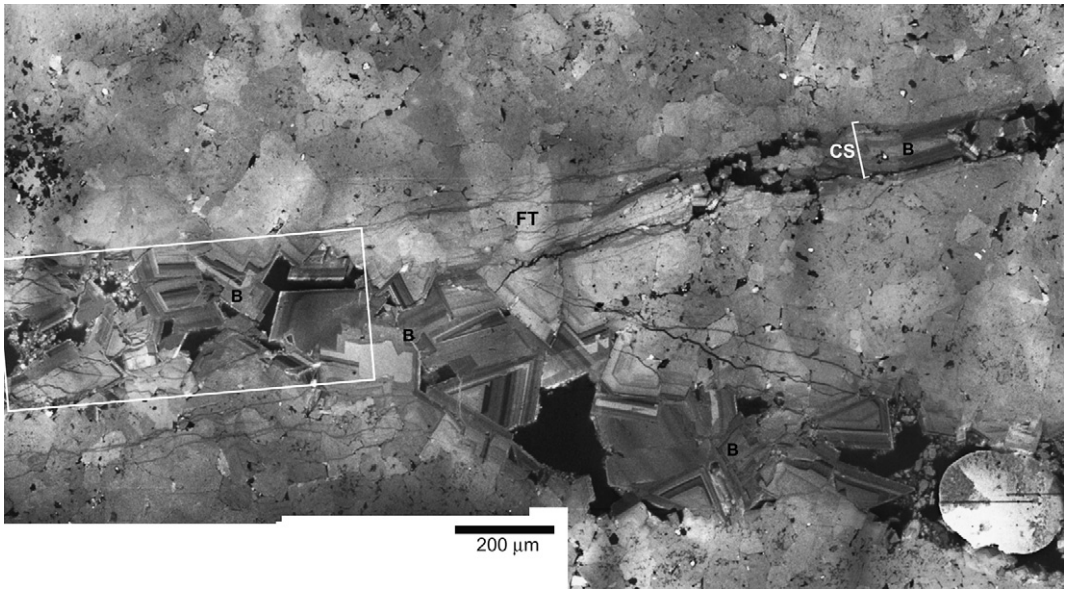

Fig. 8. Multiple sealing styles are present in a single thin section of Pennsylvanian dolostone (core sample shown in Fig. 1). The wider parts of the fractures contain porosity (black) and cement bridges (B), while the fracture tips (FT) are completely sealed. Also note crack-seal texture (CS). Box is approximate location of Fig. 4b.

observation and modeling of dolomite bridges could provide data on fracture growth rates and strain accumulation rates in sedimentary basins. In terms of prediction of hydrocarbon reservoir permeability it is important to recognize that during fracture development, dolomite cementation occurs not only within fractures but also within the host dolostone. Whereas cement bridges in open fractures will tend to prop fractures open, cement deposits within the rock mass, contemporaneous with fracture opening, will also tend to impede fracture closure under subsurface loading conditions (Laubach et al., 2004a; Olson et al., 2007). Our results suggest that cement precipitation, not present day in-situ stress, is a dominant control on stability of fracture porosity at depth in sedimentary basins.

While we chose a simple model to replicate geologically reasonable processes and conditions, we recognize that to improve upon it we would need to consider other variables. For example, we considered an end member case in which fluid is supersaturated with respect to dolomite. If the fluid was undersaturated, or if chemically reactive fluids are present, then dissolution may result (Arvidson and Mackenzie, 1999; Morse et al., 2007). Saturation indices of fluids in fractures, and kinetic inhibitors of dolomite precipitation should therefore be accounted for in a comprehensive fracture growth and sealing model. Fluid composition is also likely to influence subcritical crack propagation, thus affecting the fracture pattern and population size distribution, which will influence fracture sealing and connectivity.

9. Conclusions

Retention of fracture porosity in opening-mode fractures in dolostones is dependent on fracture aperture size. In the examples we studied fractures with apertures smaller than approximately 0.1 mm are completely sealed. Wider fractures contain anomalously thick dolomite bridges adjacent to fracture walls having only thin veneers of dolomite cement. Bridges are characteristically rhombohedral, with rhomb diagonals respectively normal and parallel to the fracture wall. Simple geometric models of crystal growth and fracture development broadly reproduce textural characteristics of dolomite cement and provide insight into the competition between rates of fracture opening and cement accumulation. The modeled textures arise because of differences in rates of growth on euhedral compared with newly fractured surfaces. Fractures become sealed by synkinematic cements when their opening rates are slower than the slowest rate of growth on any crystal surface. Conversely, fractures remain open and have a minimal absolute cement volume when opening rates exceed the fastest rate of growth on any crystal surface type. Fractures that open at rates intermediate between the slowest and fastest rates of cement growth typically retain some porosity separated by pillars or bridges of cement.

Acknowledgments

Our research on fracture and cementation processes is supported by Grant No. DE-FG02-03ER15430 Chemical Sciences, Geosciences and Biosciences Division, Office of Basic Energy Sciences, Office of Science, U.S. Department of Energy; by the Jackson School of Geology Structural Diagenesis Initiative; and by industrial associates of the University of Texas Fracture Research and Application Consortium. We are grateful to the Jackson School Geology Foundation for a seed grant specific to this project and for support of color figures. Publication is authorized by the Director, Bureau of Economic Geology, The University of Texas at Austin. We thank M. Cameron and J. Chen for insight into dolostone reservoirs and L. Bonnell, J. Hooker, J. Olson and R. Marrett for discussions. We thank special edition editor F. Agosta, reviewer P. Mollema, and an anonymous reviewer for helpful and thorough reviews.

References

Agosta, F., Prasad, M., Aydin, A., 2007. Porosity, permeability, pore structure, and capillary pressure of carbonate fault rocks, Fucino Basin (central Italy): implications for fault seal in massive limestone. Geofluids 7, 19–32.

Antonellini, M., Mollema, P.N., 2000. A natural analog for a fractured and faulted reservoir in dolomite: Triassic Sella Group, Northern Italy. AAPG Bulletin 84, 314–344.

Arvidson, R.S., Mackenzie, F.T., 1999. The dolomite problem: control of precipitation kinetics by temperature and saturation state. American Journal of Science 299, 257–288.

Becker, S.P., Eichhubl, P., Laubach, S.E., Reed, R.M., Lander, R.H., 2008. Fluid inclusion evidence for an extended opening history of fractures in quartz cemented

sandstone reservoirs (abs.). In: Belkin, H.E. (Ed.), Ninth Pan-American Conference on Research on Fluid Inclusions Programs and Abstracts, p. 5.
Bons, P.D., 2001. Development of crystal morphology during unitaxial growth in a progressively widening vein. I. The numerical model. Journal of Structural Geology 23, 865–872.
Brantley, S.L., Evans, B., Hickman, S.H., Crerar, D.A., 1990. Healing of microcracks in quartz: implications for fluid flow. Geology 18, 136–139.
Corbett, K.P., Friedman, M., Spang, J., 1987. Fracture development and mechanical stratigraphy of Austin Chalk, Texas. AAPG Bulletin 71, 17–28.
Dutton, S.P., Kim, E.M., Broadhead, R.F., Breton, C.L., Raatz, W.D., Ruppel, S.C., Kerans, C., 2005. Play analysis and digital portfolio of major oil reservoirs in the Permian Basin. In: Bureau of Economic Geology Report of Investigations No. 271. The University of Texas at Austin. CD-ROM.
Ferrill, D.A., Morris, A.P., 2008. Fault zone deformation controlled by carbonate mechanical stratigraphy, Balcones fault system, Texas. AAPG Bulletin 92, 359–380.
Gale, J.F.W., Gomez, L.A., 2007. Late opening-mode fractures in karst-brecciated dolostones of the Lower Ordovician Ellenburger Group, west Texas: recognition, characterization, and implications for fluid flow. AAPG Bulletin 91, 1005–1023.
Gale, J.F.W., Laubach, S.E., Marrett, R.A., Olson, J.E., Holder, J., Reed, R.M., 2004. Predicting and characterizing fractures in dolostone reservoirs: using the link between diagenesis and fracturing. In: Braithwaite, C.J.R., Rizzi, G., Darke, G. (Eds.), The Geometry and Petrogenesis of Dolomite Hydrocarbon Reservoirs. Geological Society, London, Special Publications, vol. 235, pp. 177–192.
Gale, J.F.W., Cameron, M.S., Reed, R.M., 2008. Fracture enhanced permeability within a crystalline porous dolostone matrix: a reservoir model in the Knox Formation, Maben gas field, Mississippi (abs.). In: AAPG 2008 Annual Convention and Exhibition Abstracts, vol. 17, p. 62.
Gomez, L.G., Laubach, S.E., 2006. Rapid digital quantification of microfracture populations. Journal of Structural Geology 28, 408–420.
Hilgers, C., Urai, J.L., 2002a. Microstructural observations on natural syntectonic fibrous veins: implications for the growth process. Tectonophysics 352, 257–274.
Hilgers, C., Urai, J.L., 2002b. Experimental study of syntaxial vein growth during lateral fluid flow in transmitted light: first results. Journal of Structural Geology 24, 1029–1043.
Hilgers, C., Koehn, D., Bons, P.D., Urai, J.L., 2001. Development of crystal morphology during unitaxial growth in a progressively widening vein: II. Numerical simulations of the evolution of antitaxial fibrous veins. Journal of Structural Geology 23, 873–885.
Hilgers, C., Kirschner, D.L., Breton, J.-P., Urai, J.L., 2006. Fracture sealing and fluid overpressures in limestones of the Jabal Akhdar dome, Oman mountains. Geofluids 6, 168–184.
Kosa, E., Hunt, D.W., 2006. Heterogeneity in fill and properties of karst-modified syndepositional faults and fractures: Upper Permian Capitan Platform, New Mexico, U.S.A. Journal of Sedimentary Research 76, 131–151.
Lander, R.H., Walderhaug, O., 1999. Porosity prediction through simulation of sandstone compaction and quartz cementation. AAPG Bulletin 83, 433–449.
Lander, R.H., Larese, R.E., Bonnell, L.M., 2008. Toward more accurate quartz cement models – the importance of euhedral vs. non-euhedral growth rates. AAPG Bulletin 92, 1537–1563.
Laubach, S.E., 1988. Subsurface fractures and their relationship to stress history in East Texas Basin sandstone. Tectonophysics 156, 37–49.
Laubach, S.E., 2003. Practical approaches to identifying sealed and open fractures. AAPG Bulletin 87, 561–579.
Laubach, S.E., Olson, J.E., Gale, J.F.W., 2004a. Are open fractures necessarily aligned with maximum horizontal stress? Earth & Planetary Science Letters 222, 191–195.
Laubach, S.E., Reed, R.M., Olson, J.E., Lander, R.H., Bonnell, L.M., 2004b. Coevolution of crack-seal texture and fracture porosity in sedimentary rocks: cathodoluminescence observations of regional fractures. Journal of Structural Geology 26, 967–982.
Laubach, S.E., Lander, R.H., Olson, J.E., Eichhubl, P., Bonnell, L.M., Marrett, R., 2006. Predicting Fracture Porosity Evolution in Sandstone. Final report, Contract No. DE-FG02-03ER15430. US Department of Energy.
Lawn, B.R., Wilshaw, T.T., 1975. Fracture of Brittle Solids. Cambridge University Press, Cambridge.
Marrett, R., Ortega, O., Kelsey, C., 1999. Extent of power-law scaling for natural fractures in rock. Geology 27, 799–802.
Mollema, P.N., Antonellini, M.A., 1999. Development of strike-slip faults in the dolomites of the Sella Group, Northern Italy. Journal of Structural Geology 21, 273–292.
Montañez, I.P., 1997. Secondary porosity and late diagenetic cements of the Upper Knox Group, Central Tennessee region: a temporal and spatial history of fluid flow conduit development within the Knox regional aquifer. In: Basin-Wide Diagenetic Patterns: Integrated Petrologic, Geochemical, and Hydrologic Considerations. SEPM, Special Publications, vol. 57, pp. 101–117.
Morse, J.W., Arvidson, R.S., Lüttge, A., 2007. Calcium carbonate formation and dissolution. Chemical Reviews 107, 342–381.
Noh, M.H., Lake, L.W., 2002. Geochemical modeling of fracture filling. In: Proceedings of the 13th Symposium on Improved Oil Recovery. Society of Petroleum Engineers, Tulsa, Oklahoma SPE 75245.
Nollet, S., Urai, J.L., Bons, P.D., Hilgers, C., 2005. Numerical simulations of polycrystal growth in veins. Journal of Structural Geology 27, 217–230.
Nollet, S., Hilgers, C., Urai, J.L., 2006. Experimental study of polycrystal growth from an advecting supersaturated fluid in a model fracture. Geofluids 6, 185–200.
Nordeng, S.H., Sibley, D.F., 1996. A crystal rate equation for ancient dolomites: evidence for millimeter-scale flux-limited growth. Journal of Sedimentary Research 66, 477–481.
Olson, J.E., Laubach, S.E., Lander, R.L., 2007. Combining diagenesis and mechanics to quantify fracture aperture distributions and fracture pattern permeability. In: Lonergan, L., Jolley, R.J., Sanderson, D.J., Rawnsley, K. (Eds.), Fractured Reservoirs. Geological Society, London, Special Publications, vol. 270, pp. 97–112.
Parris, T.M., Burruss, R.C., O'Sullivan, P.B., 2003. Deformation and the timing of gas generation and migration in the eastern Brooks Range foothills, Arctic National Wildlife Refuge, Alaska. AAPG Bulletin 87, 1823–1846.
Philip, Z.G., Jennings Jr., J.W., Olson, J.E., Laubach, S.E., Holder, J., 2005. Modeling coupled fracture-matrix fluid flow in geomechanically simulated fracture networks. SPE Reservoir Evaluation & Engineering 8, 300–309.
Reed, R.M., Milliken, K.L., 2003. How to overcome imaging problems associated with carbonate minerals on SEM-based cathodoluminescence systems. Journal of Sedimentary Research 73, 326–330.
Walderhaug, O., 1994. Precipitation rates for quartz cement in sandstones determined by fluid-inclusion microthermometry and temperature-history modeling. Journal of Sedimentary Research A64, 324–333.
Walderhaug, O., 1996. Kinetic modeling of quartz cementation and porosity loss in deeply buried sandstone reservoirs. AAPG Bulletin 80, 731–745.
Walderhaug, O., 2000. Modeling quartz cementation and porosity loss in Middle Jurassic Brent Group Sandstones of the Kvitebjørn Field, Northern North Sea. AAPG Bulletin 84, 1325–1339.
Zoback, M.D., 2007. Reservoir Geomechanics. Cambridge University Press.